RSC Advances

PAPER

View Article Online
View Journal | View Issue



Cite this: *RSC Adv.*, 2025, **15**, 16623

# New spirooxindole pyrrolidine/pyrrolizidine analogs: design, synthesis, and evaluation as an anticancer agent†

Narayanasamy Nivetha,[a] Janarthanan Venkatesan,[b] Dhanashree Murugan,[b] Loganathan Rangasamy,[b] Shu Pao Wu[c] and Sivan Velmathi *[a]

A novel series of mesitylene-based spirooxindoles were synthesized *via* the multicomponent [3 + 2] cycloaddition reaction in a greener medium. Spectroscopic techniques such as $^{1}$H and $^{13}$C NMR and HRMS analysis were carried out for the structural elucidation of all the spirooxindole derivatives. The *in vitro* cytotoxicity properties of spirooxindole analogs **4/5(a–g)** against the human lung (A549) cancer cell line exhibited encouraging outcomes. Of the fourteen synthesized spirooxindole analogs, seven compounds (**4a**, **4b**, **4e**, **4g**, **5c**, **5e**, and **5f**) showed greater potency towards the A549 lung cancer cell line. The cytotoxicity of the spirooxindole analogs was also investigated against a non-cancerous mouse embryonic fibroblast NIH-3T3 cell line. Compounds **5e** and **5f**, which exhibited better cytotoxic effect against the cancerous A549 cells (3.48 and 1.2 μM), appeared to be non-cytotoxic against the non-cancerous mouse embryonic fibroblast. Studies using Hoechst and acridine orange/ethidium bromide staining also demonstrated the apoptotic effect of the potent compounds, which decreased cell proliferation.

Received 7th March 2025
Accepted 24th April 2025

DOI: 10.1039/d5ra01632k

rsc.li/rsc-advances



## Introduction

Lung cancer poses a major threat to human health and is one of the most deadly and debilitating malignancies in the world.[1,2] Nonetheless, the 5 year survival rate for lung cancer is less than 15%, and the death rate remains high.[3] Over the past century, significant advancements in drug innovation regarding oral bioavailability and biological compatibility have been made; however, drug resistance has become a challenge for medicinal chemists. Consequently, pharmacologists and chemists are concentrating on the functional diversity of pharmacological leads,[4] nano-formulation, and the advancement of drug delivery systems,[5–7] with the objective of addressing current challenges. For this reason, it is crucial to find new therapeutic medications to treat lung cancer.

Spiroheterocyclic hybrids with pyrrolidine ring systems have been documented as an important class of potentially bioactive compounds that are frequently constructed *via* [3 + 2] cycloaddition of azomethine ylide[8–10] and possess a wide range of pharmacological activities.[11–13] The spirooxindole scaffold is a unique structure made up of two fundamental subunits. Oxindole, the first subunit, has several functions and can interact with biological targets by hydrogen bonding as either donors or acceptors. A carbocyclic or heterocyclic moiety fused with an oxindole ring at the C-3 position makes up the second unit. In addition, hybridizing the spirooxindole nucleus with other moieties has led to the development of new molecules with enhanced anticancer activity profiles. Because of its facile synthesis and easily accessible reagents, azomethine ylide is one of the most useful reactive 1,3-dipoles in the [3 + 2] cycloaddition reaction.[14,15] The most practical synthesis approach for functionalized spirooxindoles is the [3 + 2] cycloaddition of azomethine ylides with different dipolarophiles.

Mesitylene and its derivatives have gained huge attention in medicinal chemistry. Although mesitylene itself is not bioactive, its unique chemical structure providing a rigid, hydrophobic and electron-rich aromatic core makes it a valuable scaffold for drug design. The three methyl groups can act as points of substitution, enabling the attachment of bioactive moieties that interact with cancer cell lines. The advantages of mesitylene-based compounds are synthetic flexibility due to three reactive positions, lipophilicity aiding in cell membrane penetration and stability of the aromatic ring under physiological conditions.

Furthermore, the phenyl ring plays a crucial role in anticancer activity due to its chemical stability, planarity and ability to interact with biological targets. The presence and positions of

[a]*Organic and Polymer Synthesis Laboratory, Department of Chemistry, National Institute of Technology, Tiruchirappalli, 620015, Tamil Nadu, India. E-mail: velmathis@nitt.edu*

[b]*Drug Discovery Unit, Centre for Biomaterials, Cellular and Molecular Theragnostic (CBCMT), Vellore Institute of Technology, Vellore, 632014, Tamil Nadu, India*

[c]*Department of Applied Chemistry, National Yang Ming Chiao Tung University, Hsinchu, 30010, Taiwan, Republic of China*

† Electronic supplementary information (ESI) available. See DOI: https://doi.org/10.1039/d5ra01632k

substituents on the phenyl rings can affect how a drug molecule binds to a receptor, influencing its efficacy and selectivity. Substitution on the phenyl ring modifies biological activity like enhanced target selectivity, reduced toxicity and improved solubility and bioavailability. Generally, *para*-substitution enhances target affinity and creates hydrogen bond interactions



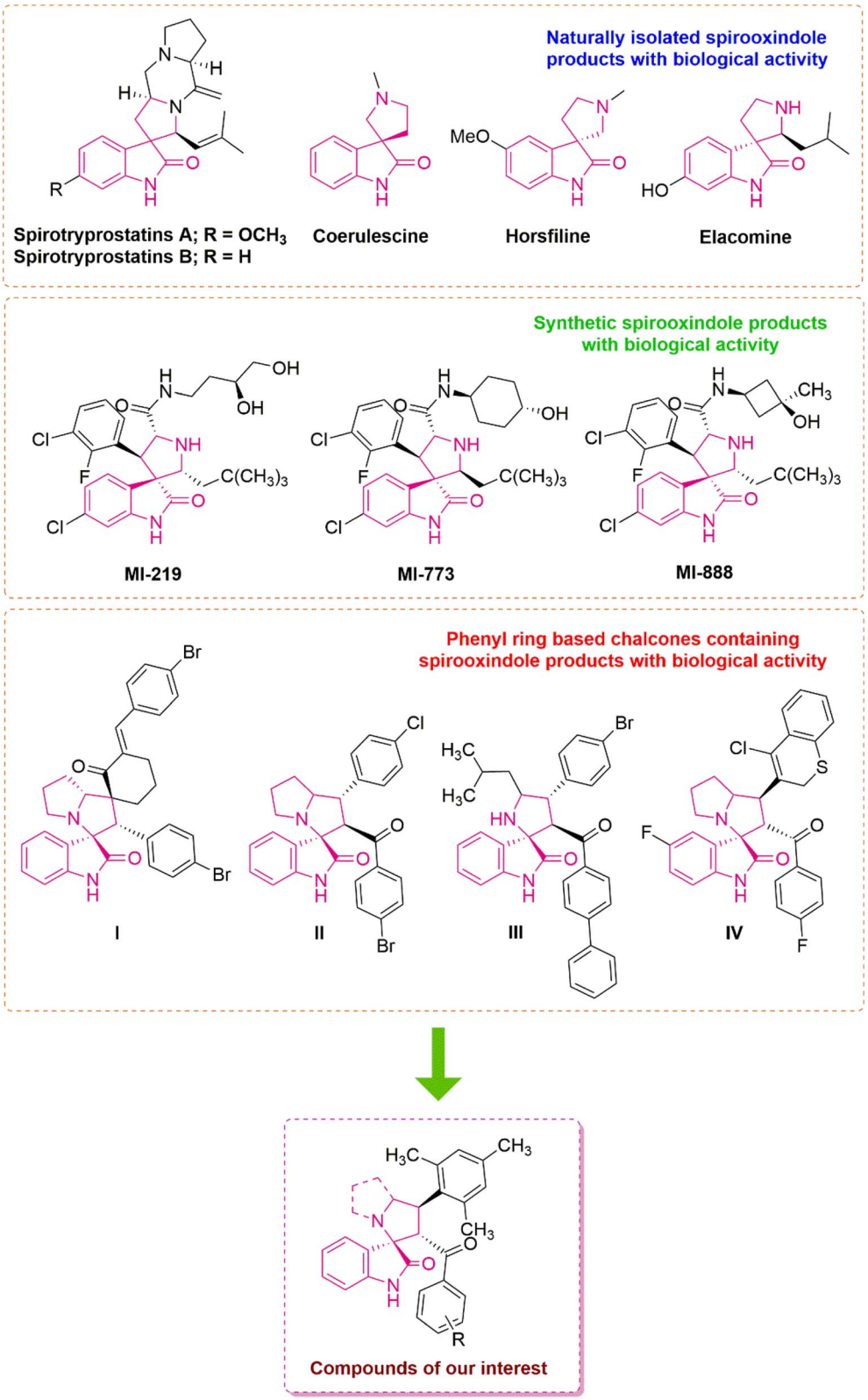


Fig. 1 Representative examples of naturally occurring and synthesized biologically active spirooxindole derivatives and rationally designed compounds of interest.

with –OH or –$NH_2$ groups whereas *meta*-substitution has the ability of tuning selectivity. In addition, the presence of –$CH_3$ and –$OCH_3$ groups modifies lipophilicity and membrane permeability. On the other hand, the presence of –Cl, –Br and –F groups increase metabolic stability and binding affinity. As a result, we have chosen mesitaldehyde and substituted acetophenones to form dipolarophiles or chalcones which undergo a cycloaddition reaction with isatin and secondary amino acids to form highly functionalized spirooxindole derivatives of interest.

Many natural spirooxindoles, such as spirotryprostatins A and B, exhibit remarkable anticancer properties.[16] Coerulescine, horsfiline, and elacomine are examples of inhibitors of the mammalian cell cycle at the G2/M interphase.[17] Among the several chemotherapeutic agents, MI-219,[18] MI-888,[19] and MI-773 (ref. 20) are some of the synthesized spirooxindole derivatives that are especially pertinent to the present study (Fig. 1). Barakat and colleagues reported a highly functionalized spirooxindole derivative and the *p*-bromophenyl arm (**I**) was identified as the most potent towards breast cancer cell lines ($IC_{50}$ values of 15.49 ± 0.04 μM).[21] Acharya's group designed and synthesized pyrrolizidine spirooxindole derivatives in which the compound with a *p*-chloro substituent (**II**) produced selective cytotoxicity against leukemia, and colon, prostate and renal cancer cell lines.[22] Parasuraman's group developed a library of spirooxindole derivatives and examined their anticancer potential against the A549 cell line.[23] The *p*-bromophenyl substituted spirooxindole derivative (**III**) showed substantial anticancer activity with $IC_{50}$ values of 15.49 ± 0.04 μM. Barakat and co-workers reported a series of thiochromene based spirocyclic hybrids and tested them against the MCF-7 and MDA-MB231 breast cancer cell lines, with the compound with a fluoro substituent (**IV**) displaying remarkable activity in the series.[24]

Motivated by these discoveries and as part of our ongoing research, we have rationally designed and synthesized a small combinatorial library of highly functionalized spirooxindoles in this work. Using a spectroscopic examination of the representative derivative, the absolute configuration was determined. Then, all derivatives were subjected to cytotoxicity screening against A549 cells to determine the selectivity using the MTT assay. Compared with cisplatin, the most promising derivatives in terms of potency and selectivity were assessed for their AO/EB and Hoechst staining tests. Additionally, the ability of the compound to reduce oxidative stress was examined by evaluating the intracellular reactive oxygen species of the most active compounds using 2′,7′-dichlorofluorescein diacetate.

## Results and discussion

We present a one-pot multicomponent 1,3-dipolar azomethine ylide cycloaddition reaction to form the mesitylene appended novel spirooxindole pyrrolidine derivative to continue our research on the synthesis of novel biologically significant heterocyclic compounds, particularly spirooxindoles.

The focus of the current study is 1,3-dipolar cycloaddition of azomethine ylides produced *in situ* through the decarboxylative condensation of substituted (*E*)-3-mesityl-1-phenylprop-2-en-1-one **1** to isatin **2** and sarcosine **3a** in ethanol, affording novel spirooxindole pyrrolidines **4** (Scheme 1).

The reaction was carried out under various conditions, and the outcomes of the reaction are summarized in Table 1. As evidenced from the results, no desired products were observed when the reaction was agitated in water at room temperature and refluxed for 24 h, respectively (Table 1, entries 1 and 2). Several solvents, including $CHCl_3$, $CH_3CN$, DMF, MeOH, EtOH, $H_2O$/MeOH, and $H_2O$/EtOH combinations were used in the process under refluxing conditions to increase the product yields (Table 1, entries 3–9). Protic solvents produced the product in good to outstanding yields, while aprotic solvents produced lesser yields. Remarkably, ethanol was found to be the best solvent that produced a high yield in a short amount of time.

Under the optimized reaction conditions, a series of 3′-benzoyl-4′-mesityl-1′-methylspiro[indoline-3,2′-pyrrolidin]-2-one derivatives **4(a–g)** were synthesized by reacting an equimolar mixture of dipolarophiles **1(a–g)**, isatin **2** and sarcosine **3** in ethanol under reflux for 2 h. After completion of the reaction (TLC), the reaction mixture was poured into ice-cold water, and the resulting solid was filtered off and purified by column chromatography to obtain pure spirooxindole pyrrolidine derivatives **4(a–g)** in 69–88% yields (Table 2). To further investigate the potential of this method, another series of (1′*R*,2′*S*,3*R*)-2′-benzoyl-1′-mesityl-1′,2′,5′,6′,7′,7*a*′-hexahydrospiro[indoline-3,3′-pyrrolizin]-2-one derivatives **5(a–g)** were synthesized by reacting an equimolar mixture of substituted dipolarophiles **1(a–g)**, isatin **2** and L-proline **3b** in ethanol under reflux for 2 h (Table 2). It was discovered that dipolarophiles with both electron-donating and electron-withdrawing substituents have good reaction rates. Dipolarophiles containing electron-donating substituents produced products in comparatively lower yields than dipolarophiles with electron-withdrawing substituents, as seen from the results displayed in Table 2. Likewise, superior product yields were noted when substituents were absent in the dipolarophile.

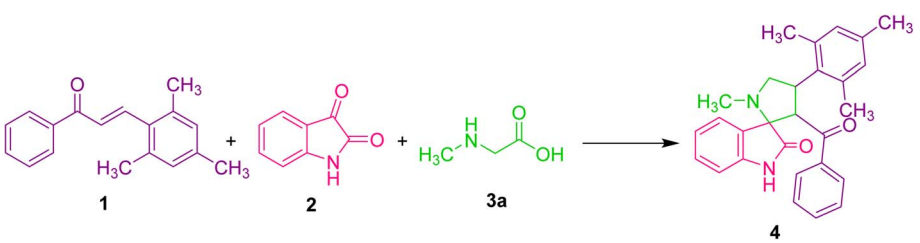


Scheme 1 Model reaction.

Table 1 Optimization of reaction conditions[a]

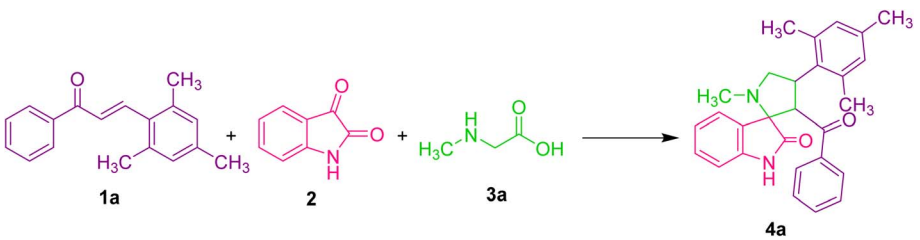


| Entry | Solvent | Temperature (°C) | Time (h) | Yield[b] (%) |
|---|---|---|---|---|
| 1 | $H_2O$ | RT[c] | 24 | NR[d] |
| 2 | $H_2O$ | 100 | 24 | NR |
| 3 | $CHCl_3$ | 63 | 12 | 44 |
| 4 | $CH_3CN$ | 84 | 12 | 55 |
| 5 | DMF | 155 | 12 | 50 |
| 6 | MeOH | 67 | 2 | 60 |
| 7 | EtOH | 80 | 2 | 73 |
| 8 | $H_2O$/MeOH | 80 | 2 | 63 |
| 9 | $H_2O$/EtOH | 80 | 2 | 66 |

[a] Reaction condition: **1a** (1.0 mmol), **2** (1.0 mmol) and **3a** (1.0 mmol) in solvent 10 mL. [b] Isolated yield. [c] RT = room temperature. [d] NR = no reaction.

The structure of new spirooxindole pyrrolidine derivatives produced by 1,3-dipolar cycloaddition of azomethine ylide was elucidated with the help of IR, $^1$H NMR, $^{13}$C NMR, and mass data as illustrated for compound **4a**. In the IR spectrum, the absorption bands at 3160 cm$^{-1}$ correspond to the NH group present in product **4a**. The absorption bands in 1712 and 1679 cm$^{-1}$ correspond to the C=O stretching frequency of ketone and amide groups, respectively. In the $^1$H NMR spectrum, the singlets at $\delta$ 1.96 and 2.62 confirmed the presence of –$CH_3$ protons of mesitylene, respectively. A singlet at $\delta$ 2.11 shows the presence of –$NCH_3$ protons of the pyrrolidine ring. A doublet and triplet at $\delta$ 3.26 and 3.43 for two protons showed the presence of pyrrolidine ring –$CH_2$ group (H-5). A triplet in the region of $\delta$ 4.93 corresponds to –CH protons (H-4 and H-3) of the pyrrolidine ring. The peaks in the range of $\delta$ 6.46–7.46 are attributed to 11 aromatic protons. The NH proton of the oxindole ring appeared as a singlet at $\delta$ 10.32. In the $^{13}$C NMR spectrum, the peaks at $\delta$ 20.70 and 21.17 correspond to methyl carbons of the mesitylene ring. The signal at $\delta$ 35.15 corresponds to –$NCH_3$ carbon. The peaks in the range of $\delta$ 39.37,

Table 2 Synthesis of spirooxindole derivatives 4(a–g) and 5(a–g)

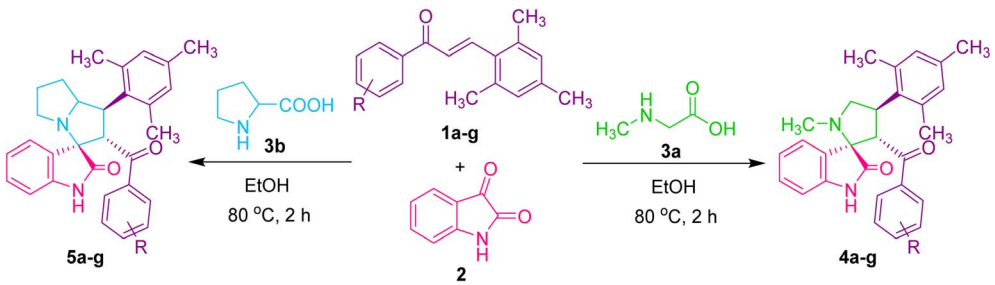


| Entry | R | Product (4) | Yield[a] (%) | Product (5) | Yield[a] (%) |
|---|---|---|---|---|---|
| 1 | H | **4a** | 73 | **5a** | 80 |
| 2 | 4-F | **4b** | 88 | **5b** | 90 |
| 3 | 4-Cl | **4c** | 85 | **5c** | 87 |
| 4 | 4-Br | **4d** | 80 | **5d** | 83 |
| 5 | 4-$CH_3$ | **4e** | 78 | **5e** | 80 |
| 6 | 3-Cl | **4f** | 80 | **5f** | 85 |
| 7 | 3-$CH_3$ | **4g** | 69 | **5g** | 70 |

[a] Isolated yield.

57.60, and 58.57 are attributed to C-4, C-5, and C-3 carbons of the pyrrolidine ring. A peak appeared at $\delta$ 74.65, confirming the spiro carbon of spirooxindole pyrrolidine in compound **4a**. Aromatic carbons resonated in the region of $\delta$ 109.73–142.04. The peaks at $\delta$ 178.21 and 197.82 confirmed the presence of two carbonyl groups. A distinguishing peak observed at *m*/*z*: 425.2269 in the high-resolution mass spectrum corresponds to the $[M + H]^+$ ion of product **4a**.

As a representative case, the strong peak in the IR spectrum of compound **5a** appeared at 3190 $cm^{-1}$, corresponding to –NH stretching, and the sharp peak in 1723 and 1678 $cm^{-1}$ corresponds to C=O stretching. In the $^1H$ NMR spectrum, the multiplets in the region of $\delta$ 1.57–1.63 and 1.67–1.73 correspond to H-6 protons of the pyrrolizidine ring. The H-7 protons appeared as a multiplet at $\delta$ 1.80–1.89. A singlet at $\delta$ 2.12 is attributed to $-CH_3$ protons. A multiplet at $\delta$ 2.36–2.39 corresponds to H-8 protons of the pyrrolizidine ring. The singlets at $\delta$ 2.60 and 2.66 confirmed the presence of $-CH_3$ protons. The multiplet, triplet, and doublet at $\delta$ 4.04–4.10, 4.39, and 5.34 correspond to methine protons (H-4, H-3, and H-5) of the pyrrolizidine ring, respectively. The 11 aromatic protons appeared in the range of $\delta$ 6.45–7.47. A singlet at $\delta$ 10.15 confirmed the presence of the –NH group of product **5a**. In the $^{13}C$ NMR spectrum, the peaks in the region of $\delta$ 20.70, 21.27, and 21.86 are attributed to $-CH_3$ carbons of the mesitylene ring. The peaks resonating at $\delta$ 28.00, 32.32, 46.88, 47.25, 61.47, and 69.72 confirmed the presence of C-7, C-6, C-4, C-8, C-3, and C-5 carbons of the pyrrolizidine ring of compound **5a**. A peak observed at $\delta$ 73.83 corresponds to the spiro carbon (C-2). Aromatic carbons appeared between the region of $\delta$ 109.99–142.39. The two carbonyl groups resonated at $\delta$ 179.54 and 197.81, respectively. A distinguishing peak observed at *m*/*z*: 451.2424 in the HRMS for the $[M + H]^+$ ion further confirms product **5a**.

A plausible reaction pathway to validate the formation of 3′-benzoyl-4′-mesityl-1′-methylspiro[indoline-3,2′-pyrrolidin]-2-one **4** is depicted in Scheme 2. The reaction of isatin **2** and sarcosine **3a** by dehydration and successive decarboxylation furnishes the azomethine ylide or 1,3-dipole. The azomethine ylide probably undergoes cycloaddition with dipolarophile **1a** *via* path **A**, furnishing **4**. The regioselectivity observed in the reaction may be explained by the fact that the electron-rich carbon of the 1,3-dipole prefers to add over the electron-deficient carbon of the α,β-unsaturated moiety of the dipolarophile **1a**, which is more encouraging due to the presence of a secondary orbital interaction (SOI)[25] which is not in path **B**. The other possible regioisomer **4′** was not observed in the reaction.

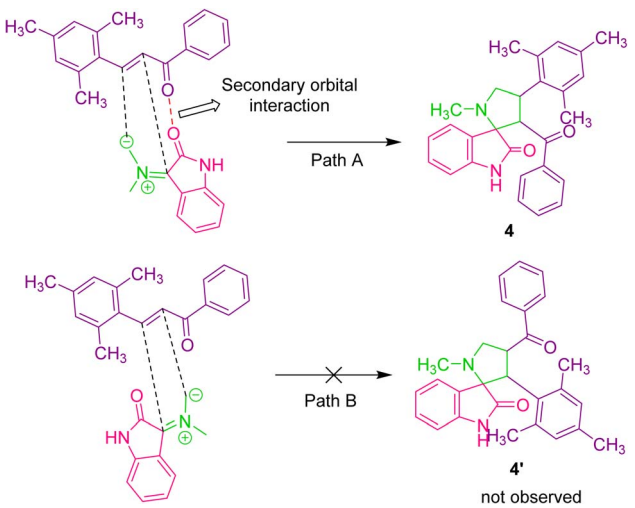


Scheme 2 Plausible reaction mechanism for the formation of spirooxindole pyrrolidine.

## Cytotoxicity studies

**MTT assay.** The cytotoxicity of compounds **4(a–g)** and **5(a–g)** was screened against the lung cancer cell line (A549 cells) and compared with the standard drug cisplatin under identical experimental conditions. All the compounds exhibited time-dependent $IC_{50}$ values, which are lower at 48 h incubation than that at 24 h, and the results are summarized in Table 3. Interestingly, they exhibit $IC_{50}$ values lower than cisplatin (22.35 ± 0.64 μM at 48 h). Compound **5f** exhibited better activity of 1.2 ± 0.412 μM at 48 h, which is nearly 13-fold higher than its activity at 24 h (16.915 ± 3.92 μM). The higher cytotoxicity of the compound may be attributed to the incorporation of the *o*-fluoro substituted aromatic ring of the chalcone moiety. Comparable cytotoxic activity was observed with compounds **5e**, **4g**, **4b**, and **4a** with the $IC_{50}$ values in the range of 3.48 ± 1.32 μM and 3.814 ± 0.02 μM. Despite the cytotoxic effects of compounds **4e**, **5g**, **5c**, **4c**, **5a**, **4d**, **5d**, and **5b**, they exhibited better activity than cisplatin. The delayed onset of action was observed with compound **4c** having a *p*-chloro group on the aromatic ring, which exhibited better cytotoxic effects at 48 h (10.26 ± 2.73 μM), whereas no activity at 24 h, even at 100 μM. The initial 24 hours might not be enough for the compound to exert its full cytotoxic effects. No substantial reduction in cell viability was observed for compound **4f** incorporated with 3-chloro substitution on the phenyl ring at 24 and 48 h, representing the lowest cytotoxicity against A549 cells. The

Table 3 *In vitro* cytotoxicity assay of synthesized compounds with cisplatin as a positive control against the A549 cell line

| Compounds | $IC_{50}$[a] at 24 h (μM) | $IC_{50}$[a] at 48 h (μM) |
|---|---|---|
| **4a** | 6.6025 ± 0.108 | 3.814 ± 0.02 |
| **4b** | 9.023 ± 2.44 | 3.22 ± 0.17 |
| **4c** | >100 | 10.26 ± 2.73 |
| **4d** | 33.53 ± 0.34 | 14.49 ± 3.18 |
| **4f** | >100 | >100 |
| **4e** | 6.929 ± 0.271 | 5.5 ± 0.5 |
| **4g** | 9.40 ± 0.611 | 3.5 ± 0.13 |
| **5a** | 28.90 ± 12.7 | 10.76 ± 1.9 |
| **5b** | 64.39 ± 9.8 | 17.39 ± 1.82 |
| **5c** | 12.90 ± 2.28 | 8.242 ± 0.34 |
| **5d** | 55.61 ± 0.18 | 13.45 ± 1.27 |
| **5e** | 15.65 ± 0.063 | 3.48 ± 1.32 |
| **5f** | 16.915 ± 3.92 | 1.2 ± 0.412 |
| **5g** | 11.06 ± 8.9 | 7.8 ± 2.3 |
| Cisplatin | >50 | 22.35 ± 0.64 |

[a] Data are mean% ± SD% of each triplicate.

cytotoxicity results of synthesized compounds and cisplatin were plotted against concentration *vs.* percentage of live cells at 24 and 48 h (Fig. S1–S4†).

**AO/EB and Hoechst staining assay.** The acridine orange/ethidium bromide (AO/EB) and Hoechst staining assays have been carried out to visualize morphological changes during the

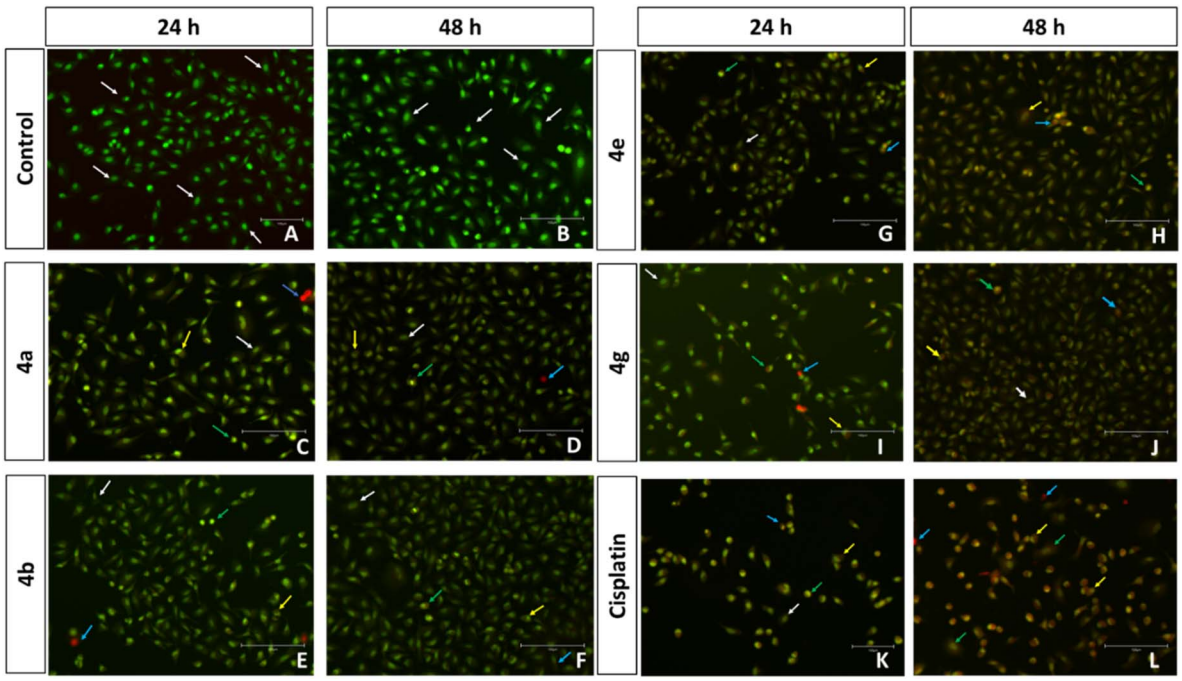


Fig. 2 Acridine orange/ethidium bromide (AO/EB) stained A549 cell line with untreated control (A and B), treated with compounds **4a** (C and D), **4b** (E and F), **4e** (G and H), **4g** (I and J), and cisplatin positive control (K and L) at 24 h and 48 h. White arrows indicate normal cells; yellow arrows indicate nuclear disintegration, chromatin condensation, and fragmentation, which are various stages of apoptosis; blue arrows indicate dead cells; and green arrows indicate swelled cells characteristic of necrosis. Scale = 150 μm, magnification = 20×.

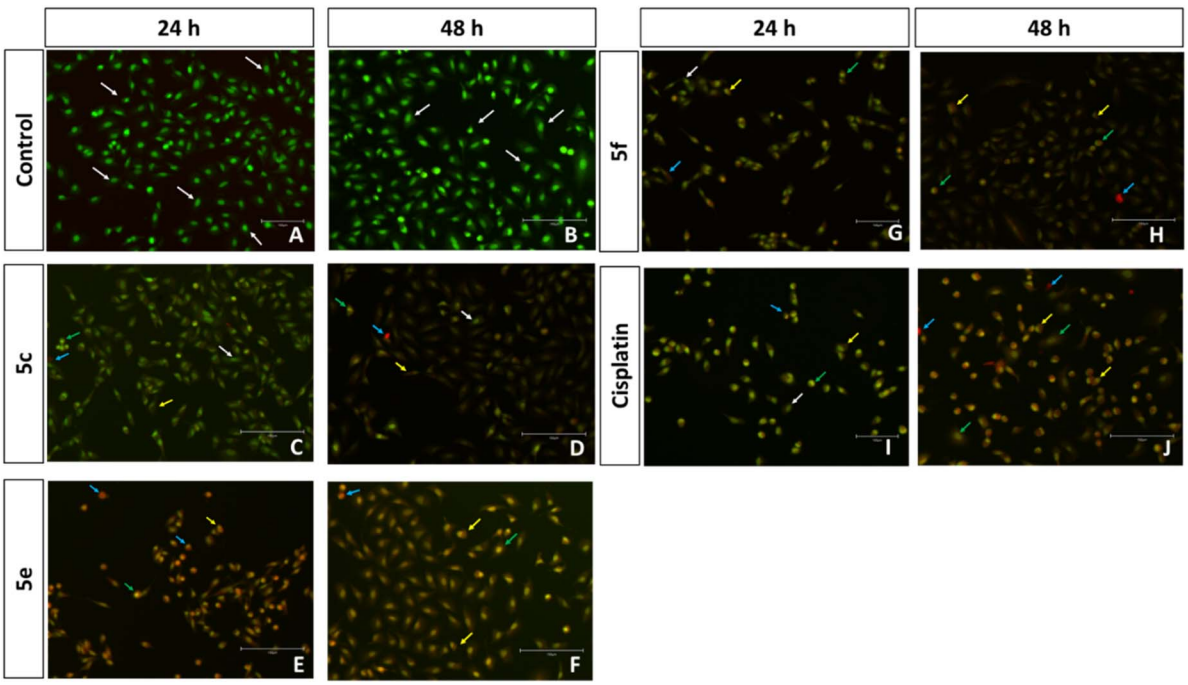


Fig. 3 Acridine orange/ethidium bromide (AO/EB) stained A549 cell line with untreated control (A and B), treated with compounds **5c** (C and D), **5e** (E and F), **5f** (G and H), and cisplatin positive control (I and J) at 24 h and 48 h. White arrows indicate normal cells; yellow arrows indicate nuclear disintegration, chromatin condensation, and fragmentation, which are various stages of apoptosis; blue arrows indicate dead cells; and green arrows indicate swelled cells characteristic of necrosis. Scale = 150 μm, magnification = 20×.

treatment of **4** and **5** series of compounds with A549 cells. Nuclear disintegration and fragmentation of the nuclear contents visualized through the Hoechst staining indicate the stages of apoptosis. The swelled cells, which appear in greenish yellow, represent the cells in the stage of early apoptosis, while the yellow and orangish cells represent late apoptosis. The swelled cells in red fluorescence represent the stage of necrosis.

Compounds **4a**, **4b**, **4e**, **4g**, **5c**, **5e**, and **5f** with better cytotoxic effects identified through MTT assays have been evaluated for the AO/EB and Hoechst staining assay and the plots were displayed in Fig. S5 and S6, ESI.† A higher number of early and late apoptotic cells were observed upon treatment with compounds **5f** and **5e** in correlation with their lower $IC_{50}$. The control group of A549 cells (control), in Fig. 2, displays uniform cell shape and strong green fluorescence, whereas the cells treated with **5e**, **5f**,

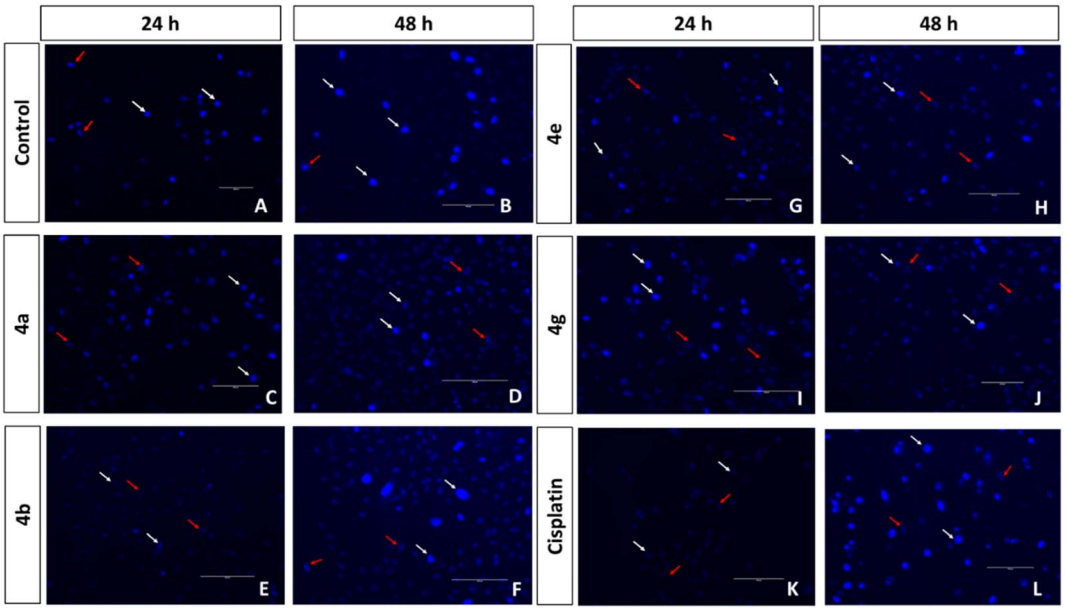


Fig. 4 Fluorescent images of Hoechst 33258 stained A549 cell line with untreated control (A and B), treated with compounds **4a** (C and D), **4b** (E and F), **4e** (G and H), **4g** (I and J), and cisplatin positive control (K and L) at 24 h and 48 h. White arrows indicate normal cells and red arrows indicate nucleus disintegrated dead cells. Scale = 150 μm, magnification = 20×.

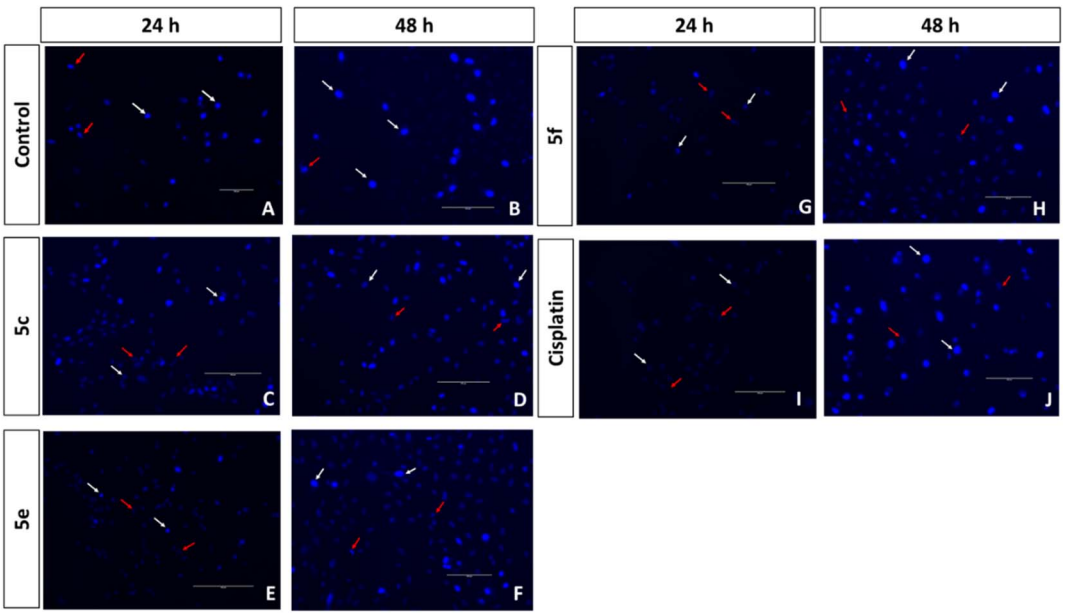


Fig. 5 Fluorescent images of Hoechst 33258 stained A549 cell line with untreated control (A and B), treated with compounds **5c** (C and D), **5e** (E and F), **5f** (G and H), and cisplatin positive control (I and J) at 24 h and 48 h. White arrows indicate normal cells and red arrows indicate nucleus disintegrated dead cells (scale = 150 μm, magnification = 20×).

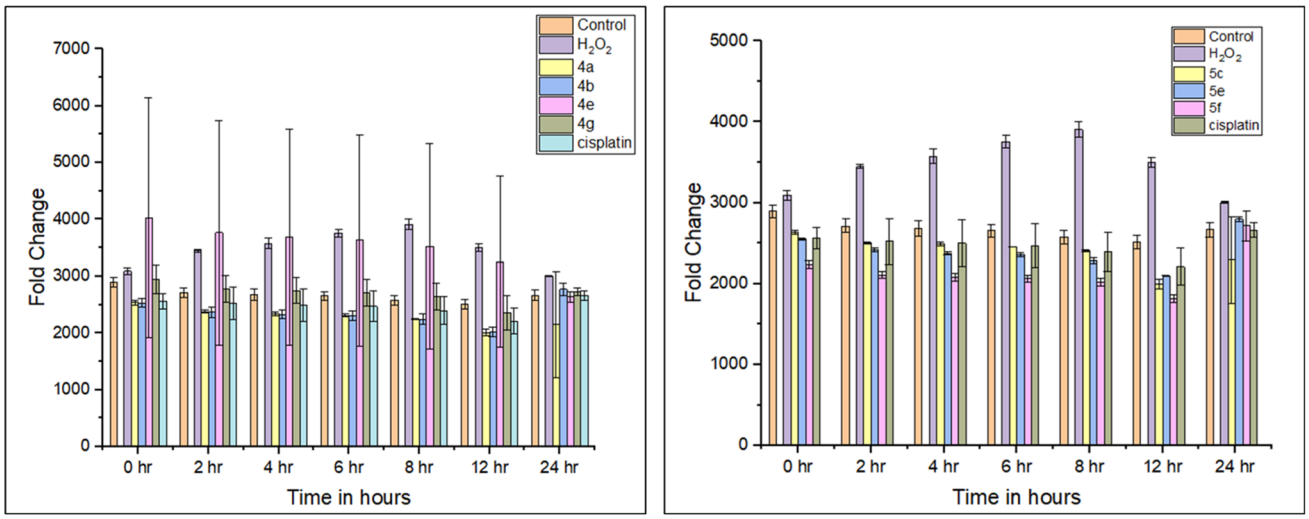


Fig. 6 ROS produced by **4a**, **4b**, **4e**, **4g**, **5c**, **5e**, **5f**, and cisplatin at 0, 2, 4, 6, 8, 12 and 24 h. The concentrations used for the studies are their respective $IC_{50}$ values. Data are mean% ± SD% of each triplicate.

and cisplatin represent distinct changes as an indication of apoptosis and cell death, such as swelling, cytoplasmic disintegration and rounding of cells within 24 and 48 h, as shown in Fig. 2–5. These studies represent the potency of compounds **5f**, **5e**, **4a**, **4b**, **4e**, **4g**, and **5c** as potential cytotoxic agents against A549 cells, which follows the order **5f** > **5e** > **4a** > **4b** > **5c** > **4e** > **4g** > cisplatin.

**Intracellular ROS generation.** The generation of reactive oxygen species (ROS) has been widely proposed as a potential mediator for induced apoptosis *via* oxidative stress. To quantify the intracellular ROS, a cell-permeable compound, 2′,7′-dichlorofluorescein diacetate (DCFH-DA), is employed for compounds **5f**, **5e**, **4a**, **4b**, **4e**, **4g**, and **5c**. Upon internalization, the non-fluorescent DCFH-DA is deacetylated by the esterase in the cell and then oxidized by the singlet oxygen generated by the compounds to fluorescent DCF. Not much difference was observed in the fluorescent intensity upon the treatment of compounds **5f**, **5e**, **4a**, **4b**, **4e**, **4g**, and **5c** compared with the untreated control group. Thus, compounds **5f**, **5e**, and **4a** exhibited apoptosis-inducing capabilities; however, it was not *via* an intracellular ROS-mediated mechanism. This may be because the spiro ring fused on the C3 position of the oxindole core with diverse heterocyclic motifs is primarily responsible for the compounds' anticancer activity.[26] The quantification of ROS in A549 cells was investigated at the $IC_{50}$ concentrations of the compounds, and the fluorescence intensity of DCF was compared with the untreated control, as shown in Fig. 6.

Table 4 *In vitro* cytotoxicity assay of drugs against NIH 3T3 cells with cisplatin as a positive control

| Compound | $IC_{50}$[a] at 24 h (μM) | $IC_{50}$[a] at 48 h (μM) |
|---|---|---|
| **4a** | >100 | 25.40 ± 3.74 |
| **4b** | >100 | 32.82 ± 5.95 |
| **4c** | >100 | >100 |
| **4d** | >100 | >100 |
| **4e** | >100 | >100 |
| **4f** | >100 | >100 |
| **4g** | >100 | 75.28 ± 0.94 |
| **5a** | >100 | 71.97 ± 4.45 |
| **5b** | >100 | 69.91 ± 1.30 |
| **5c** | >100 | 72.09 ± 0.95 |
| **5d** | >100 | 42.86 ± 1.51 |
| **5e** | >100 | >100 |
| **5f** | >100 | >100 |
| **5g** | >100 | >100 |
| Cisplatin | >50 | 24.40 ± 6.18 |

[a] Data are mean% ± SD% of each triplicate.

**Cytotoxicity of compounds in non-cancerous cells: MTT assay.** The cytotoxicity of compounds **4(a–g)** and **5(a–g)** were screened against the non-cancerous mouse embryonic fibroblast cells (NIH-3T3 cells) and compared with the currently used drug cisplatin under identical experimental conditions. The cytotoxicity assessment of the compounds was displayed in Fig. S7–S10, ESI.† All the compounds exhibited no cytotoxic effects following 24 h of the treatment, as shown in Table 4. Upon extending the interaction of the cells with the compounds to 48 h, **4a** and **4b** exhibited comparatively higher cytotoxicity with $IC_{50}$ = 25.40 ± 3.74 μM and 32.82 ± 5.95 μM, respectively. Although compounds **5d**, **5b**, **5a**, **5c**, and **4g** exhibited cytotoxicity to non-cancerous cells ($IC_{50}$ = 40 to 75 μM), their cytotoxicity was lower than that of cisplatin ($IC_{50}$ = 24.40 ± 6.18 μM). Importantly, compounds **5f** and **5e** exhibited better apoptosis against the cancerous A549 cells at their $IC_{50}$ concentration, and have no cytotoxic effects on non-cancerous NIH-3T3 cells, even following the treatment up to 48 h, indicating the selectivity of compounds **5f** and **5e** towards cancer cells.

## Conclusions

We synthesized a novel series of mesitylene-based spirooxindole derivatives *via* a cost-effective one-pot multicomponent cycloaddition reaction and evaluated their anticancer activity against A549 lung cancer cell lines. Seven compounds (**4a**, **4b**, **4e**, **4g**, **5c**, **5e** and

**5f**) exhibited $IC_{50}$ values of less than 10 μM in A549 cells. Notably, **5f** outperformed cisplatin, showing that the compound was potent and selective against the A549 lung cancer cell line. The AO/EB and Hoechst staining assays indicated that compound **5f** induces apoptosis. Compound **5f** is non-cytotoxic towards non-cancerous mouse embryonic fibroblast NIH-3T3 cells and selective towards A549 cells. Overall, we found that the viability of cancer cells decreased while that of non-cancer cells remained intact during incubation with the synthesized compound. These findings suggested that the synthesized compound may be used as a therapeutic agent for cancer chemotherapy.

## Materials and methods

### General

All chemicals and solvents were purchased from commercial suppliers and used as such. Reaction progresses were monitored by TLC using Merck silica gel 60 $F_{254}$ plates. Melting points were recorded using the Veego (VMP-DS) apparatus in open capillary tubes. $^1$H and $^{13}$C NMR spectra were run on an Agilent 400 MHz spectrometer in DMSO-$d_6$ as a solvent. Chemical shifts are given in parts per million (ppm), and the coupling constants (*J*) are given in Hertz (Hz). IR spectra were recorded on a Bruker Alpha II ATR mode spectrometer. An Agilent QTOF G6545 spectrometer was used to obtain high-resolution mass spectra. The A549 and NIH-3T3 cell lines were procured from the National Centre for Cell Science (NCCS), Pune, India. The reagents used for the *in vitro* experiments such as Dulbecco's Modified Eagle Medium (DMEM), fetal bovine serum (RM10432), 3-(4,5-dimethylthiazol-2-yl)-2,5-diphenyltetrazolium bromide (MTT), cell culture grade DMSO, acridine orange and ethidium bromide were procured from Himedia. Hoechst 33258 was obtained from Thermo Fisher Scientific. 2′,7′-Dichlorofluorescein diacetate (DCFH-DA) was procured from Sigma.

**General procedure for the synthesis of dipolarophiles 1(a–g).** Initially, to prepare dipolarophiles **1(a–g)**, a mixture of mesitaldehyde (1.0 mmol) and substituted acetophenones (1.0 mmol) was stirred in methanol (5 mL) at room temperature for 2 h in the presence of 20% KOH (5 mL). After completion of the reaction, the crude solid was filtered and washed with ice-cold water to give the pure products.

**General procedure for the synthesis of spirooxindoles 4/5(a–g).** Dipolarophiles **1(a–g)**, isatin **2**, and sarcosine **3a** or L-proline **3b** in an equimolar ratio in 5 mL of methanol were heated under reflux for 2 h. After the reaction was completed (monitored by TLC), the reaction mixture was discharged into 50 mL of ice-cold water. The obtained crude product was purified by column chromatography using hexane:ethyl acetate (80 : 20 v/v) to afford the spirooxindole pyrrolidines **4(a–g)**/pyrrolizidines **5(a–g)** in good yields.

*3′-Benzoyl-4′-mesityl-1′-methylspiro[indoline-3,2′-pyrrolidin]-2-one (**4a**).* Beige solid. Yield: 73%. Mp. 156–158 °C. IR: $\nu_{max}$ (KBr, cm$^{-1}$): 3160 (NH), 1712 (C=O), 1679 (C=O). $^1$H NMR (400 MHz, DMSO-$d_6$) $\delta_H$: 1.96 ($CH_3$) (s, 3H), 2.11 (N–$CH_3$) (s, 3H), 2.62 ($CH_3$) (s, 6H), 3.26 (H-5) (d, 1H, $J$ = 8.4 Hz), 3.43 (H-5) (t, 1H, $J$ = 8.2 Hz), 4.93 (H-3 and H-4) (t, 2H, $J$ = 10.0 Hz), 6.46 (d, 1H, $J$ = 7.6 Hz, Ar–H), 6.76 (s, 2H, Ar–H), 6.89–6.93 (m, 1H, Ar–H), 7.01–7.05 (m, 1H, Ar–H), 7.12 (d, 1H, $J$ = 7.6 Hz, Ar–H), 7.27 (t, 2H, $J$ = 7.6 Hz, Ar–H), 7.31–7.33 (m, 2H, Ar–H), 7.42–7.46 (m, 1H, Ar–H), 10.32 (NH) (s, 1H). $^{13}$C NMR (100 MHz, DMSO-$d_6$) $\delta_C$: 20.70 ($CH_3$), 21.17 ($CH_3$), 35.15 (N–$CH_3$), 39.37 (C-4), 57.60 (C-5), 58.57 (C-3), 74.65 (C-2), 109.73, 121.94, 126.32, 126.85, 127.79, 128.82, 129.36, 133.55, 133.88, 135.54, 137.17, 137.43, 142.04, 178.21 (C=O), 197.82 (C=O). HRMS (ESI) *m*/*z* [M + H]$^+$: calcd for $C_{28}H_{29}N_2O_2$: 425.2229, found: 425.2269.

*3′-(4-Fluorobenzoyl)-4′-mesityl-1′-methylspiro[indoline-3,2′-pyrrolidin]-2-one (**4b**).* White solid. Yield: 88%. Mp. 195–197 °C. IR: $\nu_{max}$ (KBr, cm$^{-1}$): 3153 (NH), 1715 (C=O), 1684 (C=O). $^1$H NMR (400 MHz, DMSO-$d_6$) $\delta_H$: 1.93 ($CH_3$) (s, 3H), 2.10 (N–$CH_3$) (s, 3H), 2.60 ($CH_3$) (s, 6H), 3.27 (H-5) (d, 1H, $J$ = 7.2 Hz), 3.39 (H-5) (t, 1H, $J$ = 7.6 Hz), 4.87–4.85 (H-3 and H-4) (m, 2H), 6.46 (d, 1H, $J$ = 7.6 Hz, Ar–H), 6.75 (m, 1H, Ar–H), 6.88–6.92 (m, 1H, Ar–H), 7.01–7.05 (m, 1H, Ar–H), 7.09 (t, 3H, $J$ = 8.6 Hz, Ar–H), 7.37–7.34 (m, 3H, Ar–H), 10.32 (NH) (s, 1H). $^{13}$C NMR (100 MHz, DMSO-$d_6$) $\delta_C$: 20.75 ($CH_3$), 21.20 ($CH_3$), 35.24 (N–$CH_3$), 39.14 (C-4), 57.75 (C-5), 58.92 (C-3), 74.77 (C-2), 109.85, 115.94 (d, $J_{CF}$ = 22.0 Hz), 122.06, 126.22, 126.85, 129.52, 130.40, 130.83 (d, $J_{CF}$ = 9.4 Hz), 135.98, 135.63, 137.50, 142.05, 178.18 (C=O), 196.56 (C=O). HRMS (ESI) *m*/*z* [M + H]$^+$: calcd for $C_{28}H_{28}FN_2O_2$: 443.2135, found: 443.2169.

*3′-(4-Chlorobenzoyl)-4′-mesityl-1′-methylspiro[indoline-3,2′-pyrrolidin]-2-one (**4c**).* White solid. Yield: 85%. Mp. 193–195 °C. IR: $\nu_{max}$ (KBr, cm$^{-1}$): 3177 (NH), 1715 (C=O), 1690 (C=O). $^1$H NMR (400 MHz, DMSO-$d_6$) $\delta_H$: 1.93 ($CH_3$) (s, 3H), 2.10 (N–$CH_3$) (s, 3H), 2.60 (CH3) (s, 6H), 3.25 (H-5) (d, 1H, $J$ = 8.0 Hz), 3.38 (H-5) (t, 1H, $J$ = 5.4 Hz), 4.86 (H-3 and H-4) (t, 2H, $J$ = 5.6 Hz), 6.46 (d, 1H, $J$ = 7.6 Hz, Ar–H), 6.75 (s, 2H, Ar–H), 6.88–6.92 (m, 1H, Ar–H), 7.01–7.05 (m, 1H, Ar–H), 7.10 (d, 1H, $J$ = 7.2 Hz, Ar–H), 7.26 (d, 2H, $J$ = 8.4 Hz, Ar–H), 7.33 (d, 2H, $J$ = 8.8 Hz, Ar–H), 10.32 (NH) (s, 1H). $^{13}$C NMR (100 MHz, DMSO-$d_6$) $\delta_C$: 21.17 ($CH_3$), 21.62 ($CH_3$), 35.64 (N–$CH_3$), 39.52 (C-4), 58.19 (C-5), 59.46 (C-3), 75.15 (C-2), 110.30, 122.51, 126.57, 127.25, 129.42, 130.00, 130.12, 134.36, 136.07, 136.32, 137.92, 138.91, 142.48, 178.53 (C=O), 197.52 (C=O). HRMS (ESI) *m*/*z* [M + H]$^+$: calcd for $C_{28}H_{28}ClN_2O_2$: 459.1839, found: 459.1879.

*3′-(4-Bromobenzoyl)-4′-mesityl-1′-methylspiro[indoline-3,2′-pyrrolidin]-2-one (**4d**).* Yellow solid. Yield: 80%. Mp. 169–170 °C. IR: $\nu_{max}$ (KBr, cm$^{-1}$): 3181 (NH), 1715 (C=O), 1690 (C=O). $^1$H NMR (400 MHz, DMSO-$d_6$) $\delta_H$: 1.95 ($CH_3$) (s, 3H), 2.12 (N–$CH_3$) (s, 3H), 2.62 ($CH_3$) (s, 6H), 3.27 (H-5) (d, 1H, $J$ = 7.2 Hz), 3.41 (H-5) (t, 1H, $J$ = 6.0 Hz), 4.87–4.89 (H-3 and H-4) (m, 2H), 6.49 (d, 1H, $J$ = 7.6 Hz, Ar–H), 6.77 (s, 2H, Ar–H), 6.90–6.94 (m, 1H, Ar–H), 7.04–7.08 (m, 1H, Ar–H), 7.11 (d, 1H, $J$ = 7.6 Hz, Ar–H), 7.20 (d, 2H, $J$ = 8.4 Hz, Ar–H), 7.49 (d, 2H, $J$ = 8.4 Hz, Ar–H), 10.33 (NH) (s, 1H). $^{13}$C NMR (100 MHz, DMSO-$d_6$) $\delta_C$: 20.76 (CH3), 21.21 (CH3), 35.23 (N–CH3), 39.10 (C-4), 57.77 (C-5), 59.01 (C-3), 74.73 (C-2), 109.89, 122.10, 126.14, 126.84, 127.73, 129.59, 129.78, 130.41, 131.96, 133.94, 135.66, 136.22, 137.50, 142.06, 178.09 (C=O), 197.31 (C=O). HRMS (ESI) *m*/*z* [M + H]$^+$: calcd for $C_{28}H_{28}BrN_2O_2$: 503.1334, found: 503.1371.

*4′-Mesityl-1′-methyl-3′-(4-methylbenzoyl)spiro[indoline-3,2′-pyrrolidin]-2-one (**4e**).* Pale yellow solid. Yield: 78%. Mp. 103–105 °C. IR: $\nu_{max}$ (KBr, cm$^{-1}$): 3180 (NH), 1712 (C=O), 1694 (C=O). $^1$H NMR (400 MHz, DMSO-$d_6$) $\delta_H$: 1.96 ($CH_3$) (s, 3H), 2.11 (N–

$CH_3$) (s, 3H), 2.23 ($CH_3$) (s, 3H), 2.61 ($CH_3$) (s, 6H), 3.28 (H-5) (d, 1H, $J$ = 8.0 Hz), 3.39–3.43 (H-5) (m, 1H), 4.89–4.91 (H-3 and H-4) (m, 2H), 6.49 (d, 1H, $J$ = 7.6 Hz, Ar–H), 6.75 (s, 2H, Ar–H), 6.91 (t, 1H, $J$ = 7.4 Hz, Ar–H), 7.04 (t, 1H, $J$ = 7.2 Hz, Ar–H), 7.08 (d, 2H, $J$ = 8.0 Hz, Ar–H), 7.14 (d, 1H, $J$ = 7.2 Hz, Ar–H), 7.27 (d, 1H, $J$ = 8.0 Hz, Ar–H), 10.33 (NH) (s, 1H). $^{13}$C NMR (100 MHz, DMSO-$d_6$) $\delta_C$: 20.69 ($CH_3$), 21.15 ($CH_3$), 21.48 ($CH_3$), 35.17 (N–$CH_3$), 39.56 (C-4), 57.62 (C-5), 58.30 (C-3), 74.79 (C-2), 109.74, 121.90, 126.31, 126.96, 127.98, 129.32, 129.41, 130.35, 134.00, 134.74, 135.51, 137.40, 142.00, 143.95, 178.19 (C=O), 197.06 (C=O). HRMS (ESI) $m/z$ [M + H]$^+$: calcd for $C_{29}H_{31}N_2O_2$: 439.2386, found: 439.2423.

*3′-(3-Chlorobenzoyl)-4′-mesityl-1′-methylspiro[indoline-3,2′-pyrrolidin]-2-one (**4f**).* White solid. Yield: 80%. Mp. 124–126 °C. IR: $\nu_{max}$ (KBr, cm$^{-1}$): 3151 (NH), 1712 (C=O), 1691 (C=O). $^1$H NMR (400 MHz, DMSO-$d_6$) $\delta_H$: 1.96 ($CH_3$) (s, 3H), 2.12 (N–$CH_3$) (s, 3H), 2.62 ($CH_3$) (s, 6H), 3.27 (H-5) (d, 1H, $J$ = 7.2 Hz), 3.41 (H-5) (t, 1H, $J$ = 6.0 Hz), 4.85–4.88 (H-3 and H-4) (m, 2H), 6.47 (d, 1H, $J$ = 7.6 Hz, Ar–H), 6.77 (s, 2H, Ar–H), 6.93 (t, 1H, $J$ = 7.4 Hz, Ar–H), 7.06 (t, 1H, $J$ = 7.8 Hz, Ar–H), 7.10–7.12 (m, 2H, Ar–H), 7.26 (d, 1H, Ar–H), 7.32 (t, 1H, $J$ = 7.8 Hz, Ar–H), 7.51 (d, 1H, $J$ = 8.4 Hz, Ar–H), 10.37 (NH) (s, 1H). $^{13}$C NMR (100 MHz, DMSO-$d_6$) $\delta_C$: 20.70 ($CH_3$), 21.16 ($CH_3$), 35.12 (N–$CH_3$), 39.10 (C-4), 57.67 (C-5), 59.26 (C-3), 74.56 (C-2), 109.80, 122.06, 126.11, 126.40, 126.68, 127.29, 129.51, 130.37, 130.76, 133.16, 133.69, 133.76, 135.60, 137.46, 138.93, 142.09, 178.07 (C=O), 197.13 (C=O). HRMS (ESI) $m/z$ [M + H]$^+$: calcd for $C_{28}H_{28}ClN_2O_2$: 459.1839, found: 459.1878.

*4′-Mesityl-1′-methyl-3′-(3-methylbenzoyl)spiro[indoline-3,2′-pyrrolidin]-2-one (**4g**).* Off-white solid. Yield: 69%. Mp. 155–157 °C. IR: $\nu_{max}$ (KBr, cm$^{-1}$): 3147 (NH), 1712 (C=O), 1676 (C=O). $^1$H NMR (400 MHz, DMSO-$d_6$) $\delta_H$: 1.96 ($CH_3$) (s, 3H), 2.111 (N–$CH_3$) (s, 3H), 2.17 ($CH_3$) (s, 3H), 2.62 ($CH_3$) (s, 6H), 3.28 (H-5) (d, 1H, $J$ = 8.0 Hz), 3.42 (H-5) (t, 1H, $J$ = 8.6 Hz), 4.87–4.92 (H-3 and H-4) (m, 2H), 6.47 (d, 1H, $J$ = 7.6 Hz, Ar–H), 6.76 (s, 2H, Ar–H), 6.90 (t, 1H, $J$ = 7.2 Hz, Ar–H), 7.01–7.05 (m, 1H, Ar–H), 7.09–7.12 (m, 2H, Ar–H), 7.15 (d, 2H, $J$ = 4.8 Hz, Ar–H), 7.24–7.25 (m, 1H, Ar–H), 10.34 (NH) (s, 1H). $^{13}$C NMR (100 MHz, DMSO-$d_6$) $\delta_C$: 20.73 ($CH_3$), 21.23 ($CH_3$), 35.19 (N–$CH_3$), 57.62 (C-5), 58.74 (C-3), 74.72 (C-2), 109.75, 121.96, 125.10, 126.44, 126.87, 128.33, 128.71, 129.34, 130.38, 133.98, 134.14, 137.26, 137.48, 138.12, 142.14, 178.31 (C=O), 197.92 (C=O). HRMS (ESI) $m/z$ [M + H]$^+$: calcd for $C_{29}H_{31}N_2O_2$: 439.2386, found: 439.2423.

*2′-Benzoyl-1′-mesityl-1′,2′,5′,6′,7′,7a′-hexahydrospiro[indoline-3,3′-pyrrolizin]-2-one (**5a**).* Beige solid. Yield: 80%. Mp. 170–173 °C. IR: $\nu_{max}$ (KBr, cm$^{-1}$): 3190 (NH), 1723 (C=O), 1678 (C=O). $^1$H NMR (400 MHz, DMSO-$d_6$) $\delta_H$: 1.57–1.63 (H-6) (m, 1H), 1.67–1.73 (H-6) (m, 1H), 1.80–1.89 (H-7) (m, 2H), 2.12 ($CH_3$) (s, 3H), 2.36–2.39 (H-8) (m, 2H), 2.60 ($CH_3$) (s, 3H), 2.66 ($CH_3$) (s, 3H), 4.04–4.10 (H-4) (m, 1H), 4.39 (H-3) (t, 1H, $J$ = 10.6 Hz), 5.34 (H-5) (d, 1H, $J$ = 12.0 Hz), 6.45 (d, 1H, $J$ = 7.6 Hz, Ar–H), 6.78 (d, 2H, $J$ = 10.0 Hz, Ar–H), 6.96 (t, 1H, $J$ = 7.2 Hz, Ar–H), 7.05–7.10 (m, 1H, Ar–H), 7.15 (d, 1H, $J$ = 7.6 Hz, Ar–H), 7.26 (d, 4H, $J$ = 4.4 Hz, Ar–H), 7.43–7.47 (m, 1H, Ar–H), 10.15 (NH) (s, 1H). $^{13}$C NMR (100 MHz, DMSO-$d_6$) $\delta_C$: 20.70 ($CH_3$), 21.27 ($CH_3$), 21.86 ($CH_3$), 28.00 (C-7), 32.32 (C-6), 46.88 (C-4), 47.25 (C-8), 61.47 (C-3), 69.72 (C-5), 73.83 (C-2), 109.99, 121.66, 127.55, 127.82, 128.78, 129.53, 129.62, 131.47, 133.49, 135.57, 137.13, 138.18, 142.39, 179.54 (C=O), 197.81 (C=O). HRMS (ESI) $m/z$ [M + H]$^+$: calcd for $C_{30}H_{31}N_2O_2$: 451.2386, found: 451.2424.

*2′-(4-Fluorobenzoyl)-1′-mesityl-1′,2′,5′,6′,7′,7a′-hexahydrospiro[indoline-3,3′-pyrrolizin]-2-one (**5b**).* Off-white solid. Yield: 90%. Mp. 186–188 °C. IR: $\nu_{max}$ (KBr, cm$^{-1}$): 3185 (NH), 1715 (C=O), 1678 (C=O). $^1$H NMR (400 MHz, DMSO-$d_6$) $\delta_H$: 1.56–1.63 (H-6) (m, 1H), 1.67–1.73 (H-6) (m, 1H), 1.78–1.91 (H-7) (m, 1H), 2.12 ($CH_3$) (s, 3H), 2.35–2.39 (H-8) (m, 2H), 2.59 ($CH_3$) (s, 3H), 2.66 ($CH_3$) (s, 3H), 4.03–4.09 (H-4) (m, 1H), 4.37 (H-3) (t, 1H, $J$ = 10.4 Hz), 5.29 (H-5) (d, 1H, $J$ = 11.6 Hz), 6.47 (d, 1H, $J$ = 7.6 Hz, Ar–H), 6.78 (d, 2H, $J$ = 8.8 Hz, Ar–H), 6.97 (t, 1H, $J$ = 7.6 Hz, Ar–H), 7.07–7.15 (m, 4H, Ar–H), 7.29–7.32 (m, 2H, Ar–H), 10.17 (NH) (s, 1H). $^{13}$C NMR (100 MHz, DMSO-$d_6$) $\delta_C$: 20.69 ($CH_3$), 21.26 ($CH_3$), 21.84 ($CH_3$), 28.05 (C-7), 32.38 (C-6), 46.72 (C-4), 47.24 (C-8), 61.80 (C-3), 69.83 (C-5), 73.88 (C-2), 110.04, 115.84 (d, $J_{CF}$ = 14.6 Hz), 121.74, 125.34, 127.48, 129.52, 129.71, 130.76 (d, $J_{CF}$ = 6.4 Hz), 131.48, 132.54, 133.87, 135.59, 136.23, 138.17, 142.35, 164.35, 166.02, 179.51 (C=O), 196.51 (C=O). HRMS (ESI) $m/z$ [M + H]$^+$: calcd for $C_{30}H_{30}FN_2O_2$: 469.2291, found: 469.2331.

*2′-(4-Chlorobenzoyl)-1′-mesityl-1′,2′,5′,6′,7′,7a′-hexahydrospiro[indoline-3,3′-pyrrolizin]-2-one (**5c**).* White solid. Yield: 87%. Mp. 164–166 °C. IR: $\nu_{max}$ (KBr, cm$^{-1}$): 3193 (NH), 1720 (C=O), 1681 (C=O). $^1$H NMR (400 MHz, DMSO-$d_6$) $\delta_H$: 1.56–1.63 (H-6) (m, 1H), 1.66–1.73 (H-6) (m, 1H), 1.81–1.89 (H-7) (m, 2H), 2.12 ($CH_3$) (s, 3H), 2.34–2.39 (H-8) (m, 2H), 2.59 ($CH_3$) (s, 3H), 2.66 ($CH_3$) (s, 3H), 4.03–4.09 (H-4) (m, 1H), 4.36 (H-3) (t, 1H, $J$ = 10.4 Hz), 5.28 (H-5) (d, 1H, $J$ = 11.6 Hz), 6.48 (d, 1H, $J$ = 7.6 Hz, Ar–H), 6.78 (d, 2H, $J$ = 8.4 Hz, Ar–H), 6.95–6.99 (m, 1H, Ar–H), 7.07–7.12 (m, 1H, Ar–H), 7.14 (d, 1H, $J$ = 7.2 Hz, Ar–H), 7.21 (d, 2H, $J$ = 8.8 Hz, Ar–H), 7.34 (d, 2H, $J$ = 8.8 Hz, Ar–H), 10.18 (NH) (s, 1H). $^{13}$C NMR (100 MHz, DMSO-$d_6$) $\delta_C$: 20.70 ($CH_3$), 21.27 ($CH_3$), 21.84 ($CH_3$), 28.05 (C-7), 32.39 (C-6), 46.65 (C-4), 47.22 (C-8), 61.92 (C-3), 69.87 (C-5), 73.84 (C-2), 110.08, 121.78, 125.29, 127.46, 128.91, 129.53, 129.63, 129.77, 131.48, 132.50, 135.62, 135.85, 136.23, 138.16, 138.36, 142.36, 179.43 (C=O), 197.05 (C=O). HRMS (ESI) $m/z$ [M + H]$^+$: calcd for $C_{30}H_{30}ClN_2O_2$: 485.1996, found: 485.2026.

*2′-(4-Bromobenzoyl)-1′-mesityl-1′,2′,5′,6′,7′,7a′-hexahydrospiro[indoline-3,3′-pyrrolizin]-2-one (**5d**).* Yellow solid. Yield: 83%. Mp. 178–180 °C. IR: $\nu_{max}$ (KBr, cm$^{-1}$): 3193 (NH), 1719 (C=O), 1682 (C=O). $^1$H NMR (400 MHz, DMSO-$d_6$) $\delta_H$: 1.56–1.62 (H-6) (m, 1H), 1.66–1.73 (H-6) (m, 1H), 1.81–1.89 (H-7) (m, 2H), 2.12 ($CH_3$) (s, 3H), 2.34–2.39 (H-8) (m, 2H), 2.59 ($CH_3$) (s, 3H), 2.66 ($CH_3$) (s, 3H), 4.03–4.09 (H-4) (m, 1H), 4.36 (H-3) (t, 1H, $J$ = 10.4 Hz), 5.28 (H-5) (d, 1H, $J$ = 11.6 Hz), 6.48 (d, 1H, $J$ = 7.6 Hz, Ar–H), 6.78 (d, 2H, $J$ = 8.8 Hz, Ar–H), 6.97 (t, 1H, $J$ = 7.4 Hz, Ar–H), 7.09 (d, 1H, $J$ = 7.6 Hz, Ar–H), 7.13 (d, 3H, $J$ = 8.8 Hz, Ar–H), 7.49 (d, 2H, $J$ = 8.4 Hz, Ar–H), 10.19 (NH) (s, 1H). $^{13}$C NMR (100 MHz, DMSO-$d_6$) $\delta_C$: 20.70 ($CH_3$), 21.27 ($CH_3$), 21.84 ($CH_3$), 28.05 (C-7), 32.38 (C-6), 46.65 (C-4), 47.22 (C-8), 61.87 (C-3), 69.86 (C-5), 73.83 (C-2), 110.08, 121.78, 125.28, 127.46, 127.58, 129.53, 129.72, 129.77, 131.48, 131.85, 132.49, 135.62, 136.17, 136.23, 138.16, 142.36, 179.41 (C=O), 197.24 (C=O). HRMS (ESI) $m/z$ [M + H]$^+$: calcd for $C_{30}H_{30}BrN_2O_2$: 529.1491, found: 529.1527.

*1′-Mesityl-2′-(4-methylbenzoyl)-1′,2′,5′,6′,7′,7a′-hexahydrospiro[indoline-3,3′-pyrrolizin]-2-one (**5e**).* Off-white solid. Yield: 80%.

Mp. 160–162 °C. IR: $\nu_{max}$ (KBr, $cm^{-1}$): 3188 (NH), 1720 (C=O), 1676 (C=O). $^1H$ NMR (400 MHz, DMSO-$d_6$) $\delta_H$: 1.56–1.63 (H-6) (m, 1H), 1.67–1.71 (H-6) (m, 1H), 1.79–1.88 (H-7) (m, 2H), 2.11 ($CH_3$) (s, 3H), 2.24 ($CH_3$) (s, 3H), 2.35–2.38 (H-8) (m, 2H), 2.59 ($CH_3$) (s, 3H), 2.65 ($CH_3$) (s, 3H), 4.04–4.09 (H-4) (m, 1H), 4.39 (H-3) (t, 1H, $J$ = 10.6 Hz), 5.32 (H-5) (d, 1H, $J$ = 11.6 Hz), 6.48 (d, 1H, $J$ = 7.6 Hz, Ar–H), 6.77 (d, 2H, $J$ = 10.4 Hz, Ar–H), 6.94–6.98 (m, 1H, Ar–H), 7.05–7.09 (m, 3H, Ar–H), 7.16 (d, 1H, $J$ = 7.2 Hz, Ar–H), 7.22 (d, 2H, $J$ = 8.4 Hz, Ar–H), 10.17 (NH) (s, 1H). $^{13}C$ NMR (100 MHz, DMSO-$d_6$) $\delta_C$: 20.69 ($CH_3$), 21.28 ($CH_3$), 21.49 ($CH_3$), 21.85 ($CH_3$), 28.02 (C-7), 32.30 (C-6), 46.98 (C-4), 47.23 (C-8), 61.10 (C-3), 69.65 (C-5), 73.92 (C-2), 109.99, 121.62, 125.49, 127.63, 128.02, 129.39, 129.52, 129.55, 131.45, 132.61, 134.66, 135.54, 136.20, 138.17, 142.35, 143.88, 179.56 (C=O), 197.00 (C=O). HRMS (ESI) $m/z$ $[M + H]^+$: calcd for $C_{31}H_{33}N_2O_2$: 465.2542, found: 465.2575.

*2′-(3-Chlorobenzoyl)-1′-mesityl-1′,2′,5′,6′,7′,7a′-hexahydrospiro [indoline-3,3′-pyrrolizin]-2-one (**5f**).* White solid. Yield: 85%. Mp. 144–146 °C. IR: $\nu_{max}$ (KBr, $cm^{-1}$): 3180 (NH), 1711 (C=O), 1679 (C=O). $^1H$ NMR (400 MHz, DMSO-$d_6$) $\delta_H$: 1.56–1.62 (H-6) (m, 1H), 1.66–1.73 (H-6) (m, 1H), 1.80–1.89 (H-7) (m, 2H), 2.13 ($CH_3$) (s, 3H), 2.35–2.39 (H-8) (m, 2H), 2.60 ($CH_3$) (s, 3H), 2.66 ($CH_3$) (s, 3H), 4.03–4.09 (H-4) (m, 1H), 4.35 (H-3) (t, 1H, $J$ = 10.4 Hz), 5.26 (H-5) (d, 1H, $J$ = 11.6 Hz), 6.47 (d, 1H, $J$ = 7.6 Hz, Ar–H), 6.79 (d, 2H, $J$ = 8.8 Hz, Ar–H), 6.98 (t, 1H, $J$ = 7.0 Hz, Ar–H), 7.03 (t, 1H, $J$ = 1.6 Hz, Ar–H), 7.09–7.14 (m, 2H, Ar–H), 7.20 (d, 1H, $J$ = 8.0 Hz, Ar–H), 7.31 (t, 1H, $J$ = 8.0 Hz, Ar–H), 7.51–7.53 (m, 1H, Ar–H), 10.20 (NH) (s, 1H). $^{13}C$ NMR (100 MHz, DMSO-$d_6$) $\delta_C$: 20.53 ($CH_3$), 21.10 ($CH_3$), 21.67 ($CH_3$), 27.82 (C-7), 32.18 (C-6), 46.48 (C-4), 47.10 (C-8), 62.06 (C-3), 69.72 (C-5), 73.59 (C-2), 109.89, 121.66, 125.10, 126.26, 127.11, 127.23, 129.36, 129.61, 130.56, 131.33, 132.28, 132.94, 133.50, 135.47, 136.10, 137.99, 138.79, 142.30, 179.28 (C=O), 197.04 (C=O). HRMS (ESI) $m/z$ $[M + H]^+$: calcd for $C_{30}H_{30}ClN_2O_2$: 485.1996, found: 485.2029.

*1′-Mesityl-2′-(3-methylbenzoyl)-1′,2′,5′,6′,7′,7a′-hexahydrospiro [indoline-3,3′-pyrrolizin]-2-one (**5g**).* Pale yellow solid. Yield: 70%. Mp. 106–108 °C. IR: $\nu_{max}$ (KBr, $cm^{-1}$): 3190 (NH), 1713 (C=O), 1680 (C=O). $^1H$ NMR (400 MHz, DMSO-$d_6$) $\delta_H$: 1.56–1.62 (H-6) (m, 1H), 1.66–1.73 (H-6) (m, 1H), 1.81–1.88 (H-7) (m, 2H), 2.12 ($CH_3$) (s, 3H), 2.17 ($CH_3$) (s, 3H), 2.36–2.39 (H-8) (m, 2H), 2.59 ($CH_3$) (s, 3H), 2.66 ($CH_3$) (s, 3H), 4.04–4.09 (H-4) (m, 1H), 4.38 (H-3) (t, 1H, $J$ = 10.4 Hz), 5.31 (H-5) (d, 1H, $J$ = 12.0 Hz), 6.46 (d, 1H, $J$ = 7.6 Hz, Ar–H), 6.78 (d, 2H, $J$ = 11.2 Hz, Ar–H), 6.96 (t, 1H, $J$ = 7.4 Hz, Ar–H), 7.02 (s, 1H, Ar–H), 7.09 (t, 2H, $J$ = 6.2 Hz, Ar–H), 7.15 (t, 2H, $J$ = 7.0 Hz, Ar–H), 7.25 (d, 1H, $J$ = 7.2 Hz, Ar–H), 10.15 (NH) (s, 1H). $^{13}C$ NMR (100 MHz, DMSO-$d_6$) $\delta_C$: 20.69 ($CH_3$), 21.21 ($CH_3$), 21.29 ($CH_3$), 21.85 ($CH_3$), 27.97 (C-7), 32.30 (C-6), 46.94 (C-4), 47.27 (C-8), 61.59 (C-3), 69.69 (C-5), 73.84 (C-2), 109.95, 121.63, 125.07, 125.50, 128.29, 128.62, 129.53, 131.46, 132.65, 134.00, 135.54, 137.20, 138.02, 142.45, 179.59 (C=O), 197.89 (C=O). HRMS (ESI) $m/z$ $[M + H]^+$: calcd for $C_{31}H_{33}N_2O_2$: 465.2542, found: 465.2573.

### *In vitro* studies

**MTT assay.** Cytotoxicity of the synthesized compounds was evaluated in A549 lung cell lines through MTT assays. The cells ($5 \times 10^3$ cells per well in 200 μL of media) were seeded into a 96 well plate and were allowed to grow for 24 h at 37 °C and 5% $CO_2$. Cells were treated with the increasing concentration of compounds for 24 h and 48 h. The study was conducted in triplicate. DMSO and media were used as a negative control, and cisplatin was used as a standard drug. After 24 h and 48 h, 20 μL of MTT reagent (5 mg $mL^{-1}$ in sterile distilled water) was added to each well, and plates were wrapped with aluminium foil and incubated for 4 h at 37 °C. The purple formazan product was dissolved by the addition of 100 μL DMSO to each well. The absorbance was measured at 595 nm using a microplate reader (TECAN INFINITE M Plex, Switzerland). Data was collected for three replicates each and used to calculate the mean. The percentage of live cells was calculated using the following formula:

$$\text{Live cells} = \frac{\text{mean OD of treated cells}}{\text{mean OD of treated cells (control)}} \times 100$$

$IC_{50}$ values were calculated using dose–response inhibition curves in GraphPad Prism.

**AO/EB staining assay.** A549 cells ($5 \times 10^4$ cells per well in 1000 μL of media) were seeded onto a 24 well plate and allowed to grow for 24 h at 37 °C and 5% $CO_2$. Cells were treated with the respective $IC_{50}$ concentration of compounds for 24 h and 48 h, respectively. A dual fluorescent staining solution (10 μL) containing 100 μg per mL AO and 100 μg per mL EB (AO/EB) was added to each of the wells. The morphology of apoptotic cells was examined, the cells were counted within 20 min using a fluorescent microscope (Invitrogen EVOS M5000), and the graphs were plotted using OriginLab software.

**Hoechst staining assay.** A549 cells ($5 \times 10^4$ cells per well in 1000 μL of media) were seeded onto 24 well plate and were allowed to grow for 24 h at 37 °C and 5% $CO_2$. Cells were treated with the respective $IC_{50}$ concentration of compounds for 24 h and 48 h, respectively. A fluorescent staining solution (10 μL) containing 100 μg per mL Hoechst was added to each of the wells. The morphology of stained cells was examined, and the cells were counted within 20 min using a fluorescent microscope (Invitrogen EVOS M5000), and the graphs were plotted using OriginLab software.

**ROS assay**

*Intracellular ROS generation.* Intracellular ROS activity was detected using a ROS indicator, 2′,7′-dichlorofluorescein diacetate (DCFH-DA), a cell-permeable non-fluorescent compound. DCFH-DA is deacetylated by esterase inside the cell and then oxidized by ROS to DCF. A549 cells ($3.0 \times 10^4$ cells per mL) were seeded in 24 well plates for 24 h. Later, selective compounds at $IC_{50}$ concentrations (24 h) and 30 μL of 100 μM $H_2O_2$ were added to each well. Sixty μL of 10 μM DCFH-DA was added to each well and incubated in the dark for 10 min. Then, fluorescence intensity was measured immediately under a fluorescence multi-plate reader (TECAN INFINITE M Plex, Switzerland) with excitation at 488 nm and emission at 510 nm. The readings were measured at an interval time of 0 h, 2 h, 4 h, 6 h, 8 h, 12 h and 24 h. The results were analyzed through OriginLab software by plotting fold change *vs.* time.

*Cytotoxicity in NIH 3T3 cells.* Cytotoxicity of the synthesized compounds was evaluated in NIH 3T3 cells through an MTT assay. The cells ($5 \times 10^3$ cells per well in 200 μL of media) were seeded into a 96 well plate and allowed to grow for 24 h at 37 °C and 5% $CO_2$. Cells were treated with increasing concentrations of compounds for 24 h and 48 h. The study was conducted in triplicate. DMSO and media were used as a negative control, and cisplatin was used as a standard drug, respectively. After 24 h and 48 h, 20 μL of MTT reagent (5 mg $mL^{-1}$ in sterile distilled water) was added to each well, and plates were wrapped with aluminium foil and incubated for 4 h at 37 °C. The purple formazan product was dissolved by the addition of 100 μL DMSO to each well. The absorbance was measured at 595 nm using a microplate reader (TECAN INFINITE M Plex, Switzerland). Data were collected for three replicates each and used to calculate the mean. The percentage of live cells was calculated from this data using the following formula:

$$\text{Percentage of live cells} = \frac{\text{mean OD treated cells}}{\text{mean OD of untreated cells (control)}} \times 100$$

$IC_{50}$ values were calculated using dose–response inhibition curves in GraphPad Prism.

## Data availability

All data supporting the findings of this research are available in the main article and the ESI.†

## Conflicts of interest

The authors declare no conflicts of interest.

## References

1 A. Leiter, R. R. Veluswamy and J. P. Wisnivesky, *Nat. Rev. Clin. Oncol.*, 2023, **20**, 624–639.
2 Z. Wang, J. Kim, P. Zhang, J. M. G. Achi, Y. Jiang and L. Rong, *Cell Insight*, 2022, **1**, 100015.
3 L. Yan, J. Ma, Y. Zhu, J. Zan, Z. Wang, L. Ling, Q. Li, J. Lv, S. Qi, Y. Cao, Y. Liu, L. Cao, Y. Zhang, Z. Qi and L. Nie, *J. Cell. Biochem.*, 2018, **119**, 3989.
4 Y. M. A. Aziz, G. Lotfy, M. M. Said, E. S. H. El-Ashry, E. S. H. El Tamany, S. M. Soliman, M. M. Abu-Serie, M. Teleb, S. Yousuf, L. R. Domingo and A. Barakat, *Front. Chem.*, 2021, **9**, 735236.
5 A. M. Omer, M. S. Ahmed, G. M. El-Subruiti, R. E. Khalifa and A. S. Eltaweil, *Pharmaceutics*, 2021, **13**, 338.
6 M. Hosny, M. Fawzy, A. M. Abdelfatah, E. F. Fawzy and A. S. Eltaweil, *Adv. Powder Technol.*, 2021, **32**, 3220–3233.
7 A. M. Omer, T. M. Tamer, R. E. Khalifa, A. S. Eltaweil, M. M. Agwa, S. Sabra, M. S. Abd-Elmonem, M. S. Mohy-Eldin and Z. M. Ziora, *Polymers*, 2021, **13**, 2428.
8 H. L. Teng, H. Huang and C. J. Wang, *Chem*, 2012, **18**, 12614–12618.
9 K. R. Braun, T. H. E. Freysoldt and F. Wierschem, *Chem. Soc. Rev.*, 2005, **34**, 507–516.
10 H. Pellissier, *Tetrahedron*, 2007, **63**, 3235.
11 (*a*) N. Lashgari and G. M. Ziarani, *ARKIVOC*, 2012, **1**, 277–320; (*b*) B. Yu, D. Q. Yu and H. M. Liu, *Eur. J. Med. Chem.*, 2015, **97**, 673–698; (*c*) C. V. Galliford and K. A. Scheidt, *Angew. Chem., Int. Ed.*, 2007, **46**, 8748–8758.
12 (*a*) C. Marti and E. M. Carreira, *Eur. J. Org Chem.*, 2003, **2003**, 2209–2219; (*b*) G. Bhaskar, Y. Arun, C. Balachandran, C. Saikumar and P. T. Perumal, *Eur. J. Med. Chem.*, 2012, **51**, 79–91; (*c*) M. Ghadi, A. Taheri and A. Abbasi, *Tetrahedron*, 2010, **66**, 6744–6748.
13 (*a*) A. Thangamani, *Eur. J. Med. Chem.*, 2010, **45**, 6120–6126; (*b*) A. I. Almansour, R. S. Kumar, N. Arumugam, A. Basiri, Y. Kia, M. A. Ali, M. Farooq and V. Murugaiyah, *Molecules*, 2015, **20**, 2296–2309.
14 (*a*) S. J. Tang, X. Zhang, J. Y. Sun, D. W. Niu and J. J. Chruma, *Chem. Rev.*, 2018, **118**, 10393–10457; (*b*) A. Shaabani, A. H. Rezayan and A. Sarvary, *Mol. Diversity*, 2011, **15**, 41–68; (*c*) N. Kielland and R. Lavilla, Synthesis of Heterocycles via Multicomponent Reactions II, *Topics in Heterocyclic Chemistry*, Springer, Berlin, Heidelberg, 2010, pp. 127–168.
15 (*a*) Y. Liu, H. Y. Hu, X. Wang, S. J. Zhi, Y. Kan and C. Wang, *J. Org. Chem.*, 2017, **82**, 4194–4202; (*b*) Z. M. Zhang, B. Xu, S. Xu, H. H. Wu and J. L. Zhang, *Angew. Chem., Int. Ed.*, 2016, **55**, 6324–6328; (*c*) E. Conde, I. Rivilla, A. Larumbe and F. P. Cossio, *J. Org. Chem.*, 2015, **80**, 11755–11767; (*d*) J. Mancebo-Aracil, C. Najera and J. M. Sansano, *Org. Biomol. Chem.*, 2013, **11**, 662–675.
16 C. B. Cui, H. Kakeya and H. Osada, *Tetrahedron*, 1996, **52**, 12651–12666.
17 C. B. Cui, H. Kakeya, G. Okada, R. Onose and H. Osada, *J. Antibiot.*, 1996, **49**, 527–533.
18 M. Zheng, J. Yang, X. Xu, J. T. Sebolt, S. Wang and Y. Sun, *Anticancer Res.*, 2010, **30**, 3321–3331.
19 Y. Zhao, S. Yu, W. Sun, L. Liu, J. Lu, D. McEachern, S. Shargary, D. Bernard, X. Li, T. Zhao, P. Zou, D. Sun and S. Wang, *J. Med. Chem.*, 2013, **56**, 5553–5561.
20 J. Lu, S. Guan, Y. Zhao, Y. Yu, Y. Wang, Y. Shi, X. Mao, K. L. Yang, W. Sun, X. Xu, J. S. Yi, T. Yang, J. Yang and J. G. Nuchtern, *Oncotarget*, 2016, **7**, 82757–82769.
21 G. Lotfy, E. S. H. E. Ashry, M. M. Said, E. S. E. Tamany, Y. M. A. Aziz, A. Al-Dhfyan, A. M. Al-Majid and A. Barakat, *J. Photochem. Photobiol., B*, 2018, **180**, 98–108.
22 R. Ghosh, J. B. Vitor, E. Mendes, A. Paulo and P. C. Acharya, *ACS Omega*, 2020, **5**, 27332–27343.
23 M. Sivanandhan, S. Ragupathy, A. Thangamani and A. Parasuraman, *Mol. Diversity*, 2024, DOI: **10.1007/s11030-024-10974-x**.
24 A. Barakat, M. S. Islam, M. Ali, A. M. Al-Majid, S. Alshahrani, A. S. Alamary, S. Yousuf and M. I. Choudhary, *Symmetry*, 2021, **13**, 1426.
25 (*a*) R. T. Pardasani, P. Pardasani, V. Chaturvedi, S. K. Yadav, A. Saxena and I. Sharma, *Heteroat. Chem.*, 2003, **14**, 36–41; (*b*) N. V. Lakshmi, P. Thirumurugan and P. T. Perumal, *Tetrahedron Lett.*, 2010, **51**, 1064–1068; (*c*) J. Li, J. Wang, Z. Xu and S. Zhu, *ACS Comb. Sci.*, 2014, **16**, 506–512.
26 B. Yu, D.-Q. Yu and H.-M. Liu, *Eur. J. Med. Chem.*, 2015, **97**, 673–698.